Optics Communications 284 (2011) 317–321

Contents lists available at ScienceDirect

Optics Communications

journal homepage: www.elsevier.com/locate/optcom

Femtosecond laser-induced mesoporous structures on silicon surface

Xianhua Wang [a], Feng Chen [a,*], Hewei Liu [a], Weiwei Liang [a], Qing Yang [b], Jinhai Si [a], Xun Hou [a]

[a] Key Laboratory for Physical Electronics and Devices of the Ministry of Education & Key Laboratory of Photonics Technology for Information, Shaanxi Province, School of Electronics and Information Engineering, Xi'an Jiaotong University, No. 28, Xianning West Road, Xi'an 710049, PR China

[b] State Key Laboratory for Manufacturing Systems Engineering, School of Mechanical Engineering, Xi'an Jiaotong University, No. 28, Xianning West Road, Xi'an 710049, PR China

ARTICLE INFO

Article history:
Received 28 March 2010
Received in revised form 12 August 2010
Accepted 18 August 2010

Keywords:
Surface microstructures
Mesoporous structures
Surface modification
Femtosecond laser pulse
Silicon

ABSTRACT

By femtosecond laser line-by-line scanning irradiating, large-scale microstructures were formed on the surface of silicon with dimensions of 1×1 mm^2. Scanning electron microscope investigations exhibited that homogeneous surface microstructures, such as directional-arranged bacilliform mesoporous structures, have been successfully prepared. The dependence of the surface morphology on laser pulse energy was analyzed, and the results indicated that the bacilliform mesoporous structures only can be textured within a certain energy range. The optical reflective spectrum measurement revealed that the presence of bacilliform mesoporous structures can significantly enhance the absorptivity of silicon at visible light range. This work would help to control the formation of surface micro/nanostructures on silicon and other materials, which has potential applications in solar energy, photoelectronics, biology and material science.

1. Introduction

Surface microstructures on silicon have attracted extensive attention in the past few decades because well-defined micro-patterned silicon has potential applications in photoelectronic devices, sensor technologies, solar cells, and so on [1–5]. Consequently, much research activity has been concentrated on controllable texturing of silicon via a versatile and efficient process. Reviewing previous works, multiple surface structures have been prepared on the silicon by various methods. For example, chemical treatments could be utilized to fabricate porous silicon which could be used as the material for the fabrication of micro-hotplates in low-power thermal sensors and thermal-effect micro-systems [6–8]. Other intriguing microstructures, such as silicon spikes, have tremendous potential applications as light absorbers for solar cells [9] and as micro-needles transdermal drug delivery [10]. The formation of the silicon spikes could be accomplished by means of laser-induced chemical etching [11–13] and plasma etching [14–16]. Furthermore, it has been reported that ripples in sub-micrometer scales would develop on the silicon surface after being irradiated by nanosecond laser pulses [17].

Recently, femtosecond laser pulses became a popular tool for texturing of solid materials, such as metals, dielectrics and semiconductors [18–20]. Femtosecond laser texturing of silicon is of interest due to its single-step process and controllable morphologies. A typical femtosecond laser-induced surface structure was subwavelength ripples. When irradiated by femtosecond laser pulses, ripples with interspacing of hundreds of nanometers grow on the silicon surface. The ripples were self-organized and the formation mechanisms might be related to the interference of incident laser light and the excited surface electromagnetic wave [21–24]. In addition, it has been proved that silicon spikes also can be obtained by femtosecond laser irradiation, which is attributed to capillary forces [25,26]. However, the isolated and individual functionalized spots with a dimension of several micrometers usually are useless for practical applications. The large-scale homogeneous surface microstructures, generally speaking, were prepared by means of chemical treatments; but chemical treatments will introduce chemical pollutions, which is unacceptable forbiological and other special applications.

In this paper, we present a fabrication of large-scale homogenous mesoporous structures on the surface of silicon wafers by a femtosecond laser scanning irradiation. By altering the processing parameters, such as incident laser energy, scanning speed, laser polarization and focal objectives, various surface structures, including the directional-arranged bacilliform mesoporous structures and island protrusions, were produced in regions with dimensions of 1×1 mm^2. We analyze the dependence of surface morphology on laser pulse energy, and believe that the bacilliform mesoporous structures only can be textured within a certain energy range. The optical reflective performances of textured areas also have been measured, which revealed the presence of bacilliform mesoporous structures could significantly enhance the visible light absorptivity of sample.

2. Experimental

The femtosecond laser resource employed in our experiments is a multi-pass Ti:sapphire amplifier, which delivered 800 nm, 30 fs pulses

* Corresponding author. Tel./fax: +86 029 82665105.
E-mail address: chenfeng@mail.xjtu.edu.cn (F. Chen).

0030-4018/$ – see front matter © 2010 Elsevier B.V. All rights reserved.
doi:10.1016/j.optcom.2010.08.039

at a repetition rate of 1 kHz (FEMTOPOWER compact Pro, FEMTOLASERS). The pulse energy could be continuously varied by a variable neutral density filter and a mechanical shutter could turn the laser on and off. The laser pulses were focused via a 10× microscope objective (Nikon, N. A. = 0.3) or a 20× microscope objective (Nikon, N. A. = 0.45). The samples used in our experiments are 400-μm thick Si (100) wafers. Before femtosecond laser irradiation, the wafers are cleaned by ultrasonic bath for 15 min in acetone and rinsed in deionized water.

The samples are positioned horizontally on a three-dimensional computer-controlled stage. After scanning irradiation according to the path shown in Fig. 1, the samples are treated by ultrasonic bath for 5 min both in acetone and deionized water in order to clean the residual ejections off the surface. Results are investigated by a scanning electron microscope (SEM, JEOL, JSM-6390A).

3. Results

The SEM images of surface microstructures induced by femtosecond laser pulses with different processing parameters are shown in Figs. 2–5.

Fig. 2 shows the micrographs of surface microstructures (1×1 mm^2) induced by horizontal polarized laser pulses in air. The incident laser pulse energy was set as 1.1 μJ, the scanning direction was parallel to the polarization orientation, and the interspacing between scanning lines was 4 μm. Respectively, the scanning speed and the employed focal microscope objective were: (a) 100 μm/s, 10× (N. A. = 0.3); (b) 50 μm/s, 10× (N. A. = 0.3); and (c) 100 μm/s, 20× (N. A. = 0.45).

Fig. 3 shows the micrographs of surface microstructures (1×1 mm^2) induced by vertical polarized laser pulses in air. The incident laser pulse energy was set as 1.1 μJ, and the laser pulses were focused via a 10× (N. A. = 0.3) microscope objective; the scanning direction was perpendicular to the polarization orientation. Respectively, the scanning speeds and the intervals were: (a) 100 μm/s, 4 μm; (b) 50 μm/s, 4 μm; and (c) 100 μm/s, 8 μm.

Fig. 4 shows the micrographs of surface microstructures (1×1 mm^2) induced by 45° polarized laser pulses in air. The incident laser pulse energy was set as 1.1 μJ, and the laser pulses were focused via a 10× (N. A. = 0.3) microscope objective; the polarization orientation was 45° to the scanning direction. Respectively, the scanning speeds and the intervals were: (a) 100 μm/s, 4 μm; (b) 50 μm/s, 4 μm; and (c) 100 μm/s, 8 μm.

Fig. 5 shows the micrographs of surface microstructures (200×100 μm^2) induced by horizontal polarized laser pulses in air with much higher incident laser energy densities. The laser pulses were focused via a 10× (N. A. = 0.3) microscope objective, the scanning direction was parallel to the polarization orientation, and the intervals between scanning lines were 2 μm. For Fig. 5(a), the incident laser pulse energy was set as 2.5 μJ, and the scanning speed was 160 μm/s; for Fig. 5(b), the incident laser pulse energy was 3.5 μJ and the scanning speed was 80 μm/s.

Fig. 6 shows the reflective spectrums of untreated area compared to the micro-structured areas shown in Fig. 2(a), Fig. 3(a) and Fig. 4(a). The light resource is a board-band light source (UV/VIS light source, DT 1000CE, Analytical Instrument Systems Inc.), and the incident light energies and angles are kept as under the same measurement conditions.

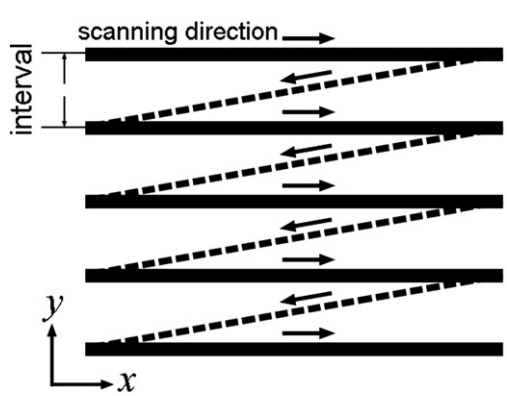

Fig. 1. The illustration of scanning path. The scanning path is zigzag: during the process, the laser pulses were irradiated horizontally along *x* direction; after reaching the end point of one scanning line, a mechanical shutter will occlude the laser beam and the stage moves the sample to the start point of next scanning line. The solid lines denote irradiated lines and the dash lines represent the un-irradiated lines.

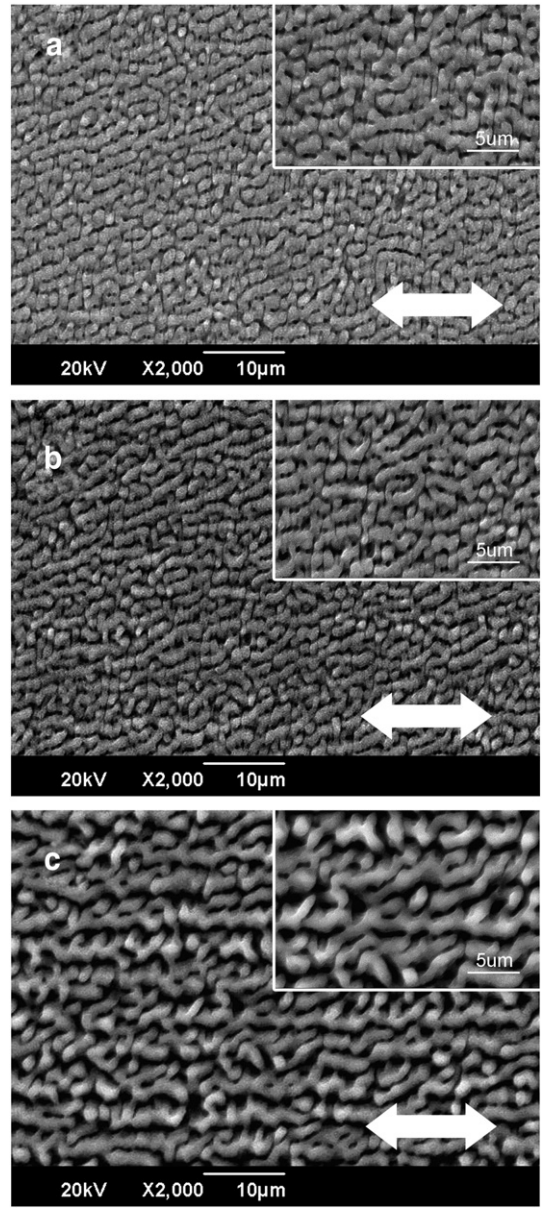

Fig. 2. The SEM images of surface microstructures (1×1 mm^2) induced by horizontal polarized laser pulses in air. The incident laser pulse energy was set as 1.1 μJ, the scanning direction was parallel to the polarization orientation, and the interval was 4 μm. Respectively, the scanning speed and the employed focal microscope objective were: (a) 100 μm/s, 10× (N. A. = 0.3); (b) 50 μm/s, 10× (N. A. = 0.3); and (c) 100 μm/s, 20× (N. A. = 0.45). The insert in each figure was the higher magnification image and the white arrow represented laser polarization.

4. Discussion

Comparing with the femtosecond laser-induced ripples or spikes reported in the previous works, the microstructures induced in our

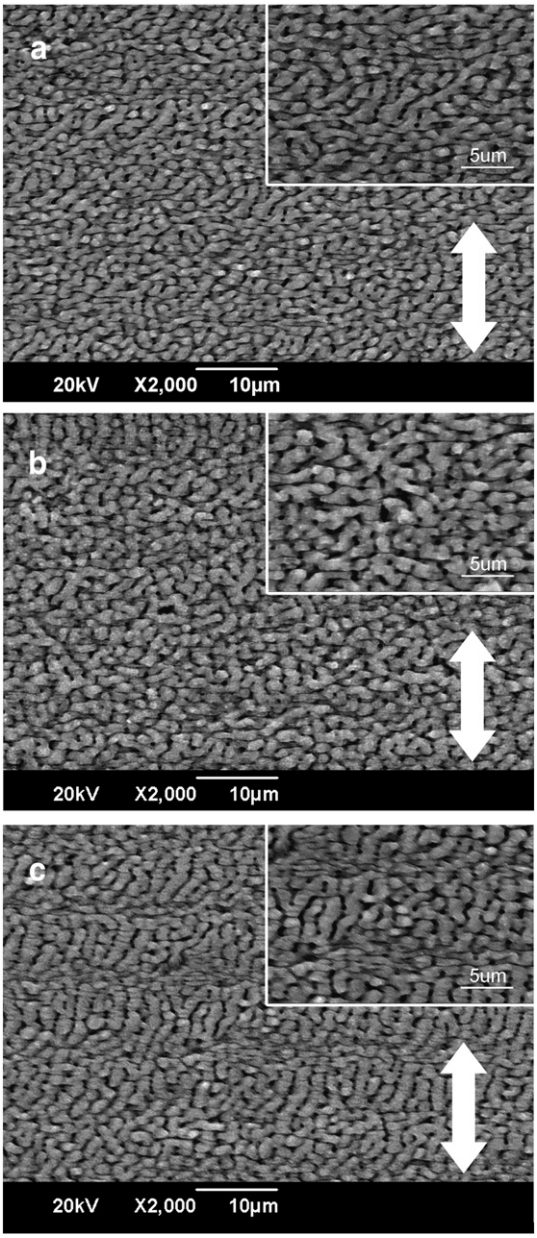

Fig. 3. The SEM images of surface microstructures (1×1 mm^2) induced by vertical polarized laser pulses in air. The incident laser pulse energy was set as 1.1 μJ, and the laser pulses were focused via a 10× (N. A. = 0.3) microscope objective; the scanning direction was perpendicular to the polarization orientation. Respectively, the scanning speeds and the intervals were: (a) 100 μm/s, 4 μm; (b) 50 μm/s, 4 μm; and (c) 100 μm/s, 8 μm. The insert in each figure was the higher magnification image and the white arrow represented laser polarization.

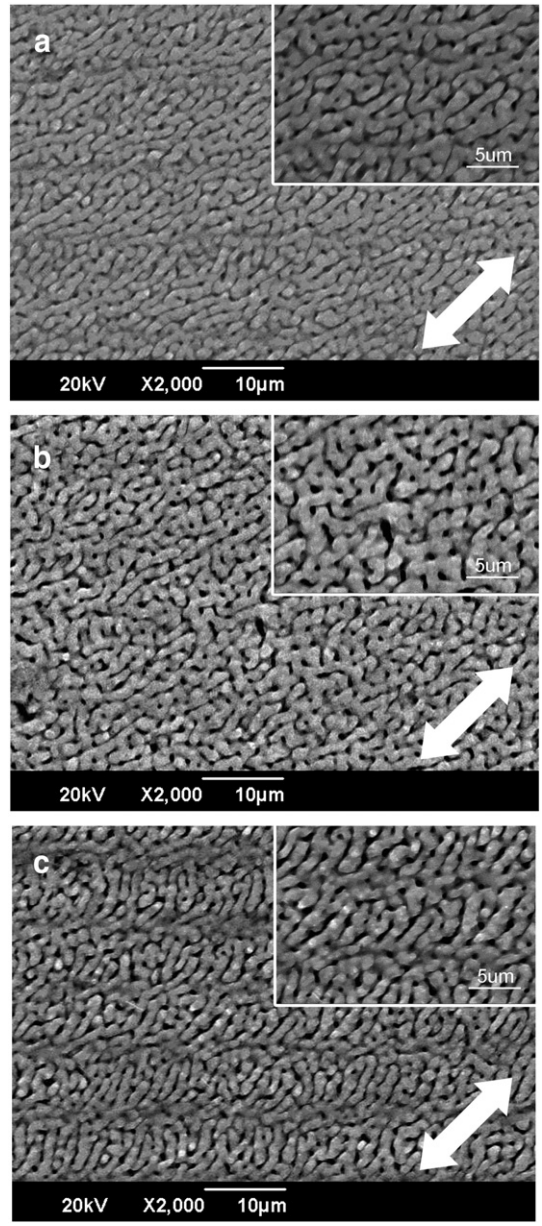

Fig. 4. The SEM images of surface microstructures (1×1 mm^2) induced by 45° polarized laser pulses in air. The incident laser pulse energy was set as 1.1 μJ, and the laser pulses were focused via a 10× (N. A. = 0.3) microscope objective; the scanning direction was perpendicular to the polarization orientation. Respectively, the scanning speeds and the intervals were: (a) 100 μm/s, 4 μm; (b) 50 μm/s, 4 μm; and (c) 100 μm/s, 8 μm. The insert in each figure was the higher magnification image and the white arrow represented laser polarization.

experiments are closer to directional-arranged bacilliform mesoporous structures (DABMS), as shown in Figs. 2–4. In Refs. [27,28], the similar structures formed in the center of ablation craters surrounded by the ripples. The formation of this type of morphology is related to the Gaussian energy distribution of laser pulses. For a Gaussian laser pulse, the energy density in the center is much higher than the periphery region, which will lead to the formation of two distinct types of microstructures: DABMS textured in higher energy density region and ripples formed in lower energy density district. It indicates that the threshold energy of the formation of DABMS is higher than that of the ripples. However, when the incident laser pulse energy further increases, the surface microstructures such as island protrusions appear in the laser-treated areas, as shown in Fig. 5(b). The surface morphology depends on the pulse energy reveals that the formation mechanisms of these microstructures is related to a series of processes, such as interference, thermal melting and resolidification of materials, shockwave effects, etc. When laser pulse energy is slightly above the ablation threshold, the interference between incident laser pulses and the surface plasmons dominates the texturing process, and the ripples form. With the pulse energy increasing, the thermal effects and shockwave effects are intensified and cannot be neglected; they compete with the interference mechanism, and result in the formation of DABMS instead of ripples. The island protrusions are caused by the thermal effects and shockwave effects due to excessive energy depositions. In that case, the interference effects can be disregarded and the surface of the solid materials will be melted, the island protrusions are produced by shockwave effects, capillary forces and resolidification of the

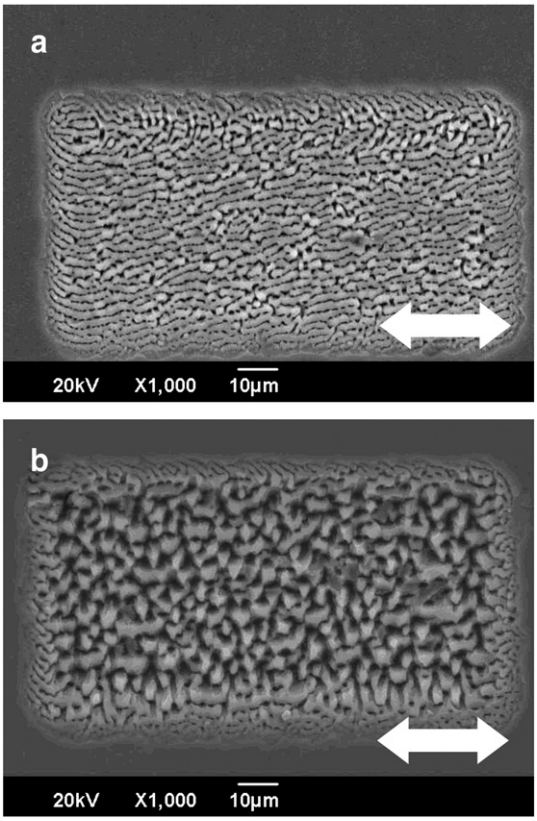

Fig. 5. The SEM images of the surface micro-morphologies ($200\times100\ \mu m^2$) induced by higher laser energy influence. The laser pulses were focused via a 10× (N. A. = 0.3) microscope objective, the scanning direction was parallel to the polarization orientation, and the interval was 2 μm. (a) The sample irradiated by the laser with pulse energy of 2.5 μJ at the speed of 160 μm/s. (b) The sample irradiated by the laser with pulse energy of 3.5 μJ at the speed of 80 μm/s. The white arrows represented laser polarization.

ejections. Consequently, the pulse energy plays a key role in the formation of microstructures.

Fig. 2(a), Fig. 3(a) and Fig. 4(a) show the influence of the laser polarization on the surface morphologies. The pulse energy and the scanning speed are 1.1 μJ and 100 μm/s, respectively. Between these SEM images, very few apparent morphological distinctions can be observed, which at the same time proves that the morphology of these structures are mainly related to the pulse energy and the threshold for texturing DABMS is higher than the ablation threshold. When laser pulse energy is slightly exceeded the ablation threshold, the formed microstructures, such as ripples, are perpendicular to the polarization orientation of laser pulses. But if the pulse energy is much higher than the ablation threshold of sample, the polarization-dependent of the microstructures are breakdown, as mentioned above, which will result in texturing of polarization-independent surface microstructures. Moreover, the reflective spectrums of them are also similar, almost down to 30% within the wavelength range from 350 nm to 800 nm compared to the untreated area, as shown in Fig. 6, which indicated that the micro-structured surfaces have enhanced the absorption in the wavelength range of visible lights. The enhancement of the absorption can be explained by significant increase of the surface area due to the formation of surface microstructures, which presents our works have promising applications in the preparation of electron and photon absorbers.

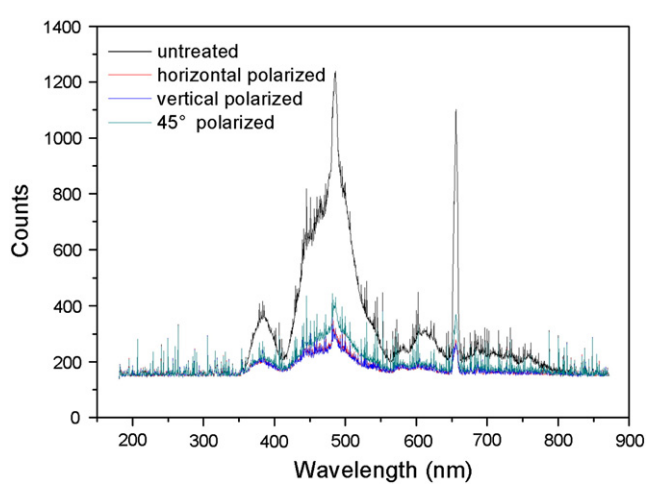

Fig. 6. The reflective spectrums of untreated area compared to the micro-structured areas shown in Fig. 2(a), Fig. 3(a) and Fig. 4(a). The incident wavelength ranged from 180 nm to 870 nm.

Fig. 2(b), Fig. 3(b) and Fig. 4(b) also show the polarization independency of the surface morphologies. The pulse energy and the scanning speed are 1.1 μJ and 50 μm/s, respectively. The similarity of them reconfirmed our analysis aforementioned. The decrease of the scanning speed would increase the number of shots deposited in a unit area, which will intensify the modification of surface morphology. Moreover, decreasing the diameter of focal spot will increase the energy density of single pulse; when we use a higher N. A. objective, laser energy concentration will increase the surface roughness. Fig. 2(c) shows the surface morphology induced by laser irradiation with pulse energy and the scanning speed were 1.1 μJ and 100 μm/s, and the laser pulses were focused via an 20× objective with N. A. = 0.45. In a short, we can control the depth of surface microstructures for different specifications and destinations.

When the intervals between the scanning lines closed to the diameter of focal spot, the deposited energy intensity will be uneven in *y*-axis direction. However, if the interval between scanning lines was been chosen properly to ensure the fluctuations were confined within a certain range, the processing efficiency will be improved without surface microstructure deformation. Fig. 3(c) and Fig. 4(c) show the surface microstructures formed by the laser beam scanning at the speed of 100 μm/s with interval of 8 μm. The experimental results revealed the microstructures in the irradiated region were quasi-uniform, and the influence of surface morphology on larger interval has arisen.

5. Conclusions

In summary, we have successfully prepared homogeneous mesoporous structures on the surface of silicon wafers via femtosecond laser pulses irradiation scanning with dimension of $1\times1\ mm^2$. The morphologies of the surface structures can be controlled by processing parameters. We analyze the dependence of surface morphology on laser pulse energy, and believe the bacilliform mesoporous structures only can be textured within a certain energy range. The influences of the surface morphology on the processing parameters have been discussed. After irradiation, the roughness and the visible light absorption performances of the sample have been modified significantly. Compared to other methods, femtosecond laser irradiation has the advantages of single-step process, controllable morphologies and without chemical pollutions, which is convenient to implement surface modification on various materials, especially for the biological materials.

Acknowledgments

The authors gratefully acknowledge the financial support for this work provided by the National Science Foundation of China under the grant nos. 60678011 & 10674107 and the National High Technology R&D Program of China under the grant no. 2009AA04Z305.

References

[1] Cheng Mu, Yuxiang Yu, Wei Liao, Xinsheng Zhao, Dongsheng Xua, Xihong Chen, Dapeng Yu, Appl. Phys. Lett. 87 (2005) 113104.
[2] M.J. Toohey, Sens. Actuators B 105 (2005) 232.
[3] Yuheng Zhang, Xinjian Li, Lei Zheng, Qianwang Chen, Phys. Rev. Lett. 81 (1998) 1710.
[4] C.C. Striemer, P.M. Fauchet, Appl. Phys. Lett. 81 (2002) 2980.
[5] Y. Nishimoto, K. Namba, Sol. Energy Mater. Sol. Cells 61 (2000) 393.
[6] Tsutomu Shimizu-Iwayama, Setsuo Nakao, Kazuo Saitoh, Appl. Phys. Lett. 65 (1994) 1814.
[7] G. Ghislotti, B. Nielsen, P. Asoka-Kumar, K.G. Lynn, A. Gambhir, L.F. Di Mauro, C.E. Bottani, J. Appl. Phys. 79 (1996) 8660.
[8] A.J. Kenyon, P.F. Trwoga, C.W. Pitt, G. Rehm, J. Appl. Phys. 79 (1996) 9291.
[9] P.B. Clapham, M.C. Hutley, Nature 244 (1973) 281.
[10] Sebastien Henry, Devin V. Mcallister, Mark G. Allen, Mark R. Prausnitz, J. Pharm. Sci. 87 (1998) 922.
[11] Tsing-Hua Her, Richard J. Finlay, Wu. Claudia, Shrenik Deliwala, Eric Mazur, Appl. Phys. Lett. 73 (1998) 1673.
[12] T.-H. Her, R.J. Finlay, C. Wu, E. Mazur, Appl. Phys. A 70 (2000) 383.
[13] A.J. Pedraza, J.D. Fowlkes, D.H. Lowndes, Appl. Phys. Lett. 74 (1999) 2322.
[14] K. Seeger, R.E. Palmer, Appl. Phys. Lett. 74 (1999) 1627.
[15] T. Tada, T. Kanayama, K. Koga, K. Seeger, S.J. Carroll, P. Weibel, R.E. Palmer, Microelectron. Eng. 41/42 (1998) 539.
[16] X.D. Bai, Zhi Xu, S. Liu, E.G. Wang, Sci. Tech. Adv. Mat. 6 (2005) 804.
[17] P.M. Fauchet, A.E. Siegman, Appl. Phys. Lett. 40 (1982) 824.
[18] Satoshi Kawata, Hong-Bo Sun, Tomokazu Tanaka, Kenji Takada, Nature 412 (2001) 697.
[19] B.N. Chichkov, C. Momma, S. Noltevon, F. Alvensleben, A. Tünnermann, Appl. Phys. A 63 (1996) 109.
[20] J. Ihlemann, B. Wolff, R. Simon, Appl. Phys. A 54 (1992) 363.
[21] D.C. Emmony, R.P. Howson, L.J. Willis, Appl. Phys. Lett. 23 (1973) 598.
[22] J.E. Sipe, J.F. Young, J.F. Preston, H.M. van Driel, Phys. Rev. B 27 (1983) 1141.
[23] S.E. Clark, D.C. Emmony, Phys. Rev. B 40 (1989) 2031.
[24] A.M. Bonch-Bruevich, M.N. Libenson, V.S. Makin, V.V. Trubaev, Opt. Eng. 31 (1992) 718.
[25] C.H. Crouch, M.Y. Shen, J.E. Carey, E. Mazur, 2002 MRS Fall Meeting, Symposium KK 3.4, 2002.
[26] M.Y. Shen, C.H. Crouch, J.E. Carey, R. Younkin, E. Mazur, M. Sheehy, C.M. Friend, Appl. Phys. Lett. 82 (2003) 1715.
[27] T. Matsumura, A. Kazama, T. Yagi, Appl. Phys. A 81 (2005) 1393.
[28] J.M. Li, J.T. Xu, Laser Phys. 19 (2009) 121.